J. Fluid Mech. (1979), *vol.* 93, *part* 4, *pp.* 609–630
Printed in Great Britain

An experimental study of the effects of wall conductivity, non-uniform magnetic fields and variable-area ducts on liquid metal flows at high Hartmann number. Part 1. Ducts with non-conducting walls

By RICHARD J. HOLROYD
Department of Engineering, University of Cambridge†

(Received 25 October 1978)

The results are presented of an experimental investigation of the flow of mercury along straight, circular and rectangular non-conducting ducts situated in a magnetic field that is uniform except over a short length of the duct where its value decreases by 50 %. Magnitudes of the field strength and mean velocity are such that the Hartmann number M is large, the interaction parameter $N \approx M^{\frac{1}{2}}$ and the magnetic Reynolds number $Rm \ll 1$. In all but one respect this is the prototype problem analysed by Holroyd & Walker (1978): their analysis required that $N \gg M^{\frac{1}{2}}$.

Distributions of pressure, electric potential and velocity are measured, the latter by hot-film probes. Qualitative agreement with the theoretical predictions is obtained in so far as a pressure drop of O(duct radius × fully-developed flow pressure gradient × $M^{\frac{1}{2}}$) occurs over the non-uniform field region and, in the circular duct, the fluid can be seen to migrate towards the centre of the duct upstream and downstream of the non-uniform field region but in that region this tendency is reversed.

Similar effects appear to occur in the rectangular duct.

1. Introduction

The main theme of this paper is an experimental investigation of the flow along a uniform bore circular pipe of radius a subjected initially to the influence of a uniform transverse magnetic field B_0 whose strength decreases to $\frac{1}{2}B_0$ further along the duct over a short length. Magnitudes of the flux density and mean velocity V are such that the Hartmann number $M[= aB_0(\sigma/\eta)^{\frac{1}{2}}]$ and interaction parameter $N(= aB_0^2\sigma/\rho V = M^2/Re$, where Re is the Reynolds number of the flow) are large and the magnetic Reynolds number $Rm\,(= \mu\sigma Va)$ is very small. Here σ, η, ρ and μ represent the conductivity, viscosity, density and permeability of the fluid respectively. This is the prototype problem analysed by Holroyd & Walker (1978) (hereafter referred to as H&W). In such cases there is a longitudinal, recirculating current flow which augments the pressure gradient upstream of the non-uniform field region and gives rise to a pressure drop of $O(a \times$ fully-developed flow pressure gradient $\times M^{\frac{1}{2}})$ while there is an inter-related distortion of the fully-developed flow in which the fluid hugs those walls of the duct where the field lines are tangential in the non-uniform region. When inertial effects are ignored, which requires $N \gg M^{\frac{1}{2}}$, these effects are expressed over

† Present address: Department of Engineering Science, University of Oxford.

large $O(aM^{\frac{1}{2}})$ distances *upstream and downstream* of the non-uniform field region. Similar effects should occur in a duct whose cross-sectional area increases and is situated in a uniform, transverse field (Walker & Ludford 1974). The governing factor of these effects is the change in magnitude of the induced electric field $\mathbf{v} \wedge \mathbf{B}$ along the duct ($\mathbf{v}$ and $\mathbf{B}$ representing the velocity field and magnetic field).

A similar but less extensive study of the flow in a rectangular duct widens the scope of the investigation. From a theoretical viewpoint this is a singular case not covered by H&W's theory and the condition for an inertialess flow is much stricter, namely $N \gg M^{\frac{3}{2}}$.

Apart from their intrinsic academic interest, especially in relation to H&W's work, it is hoped that these studies will prove useful in estimating the power required to circulate the liquid metal coolant in some designs for nuclear fusion reactors (Hunt & Holroyd 1977).

Phenomena like those described above have often been observed in experiments devoted to fully developed flows where the flow enters and leaves the region of uniform magnetic field. However, these cases differ in one important detail from the present study in that part of the recirculating current flow is in regions of zero magnetic flux density and so it cannot influence the flow. Moreover, inertial stresses must play an important role in such examples since N must have a low value (i.e. $N \lesssim M^{\frac{1}{2}}$) over at least some part of the flow. Shercliff (1956*a*, *b*) has shown that in low-N situations the fully-developed flow is realized within a distance $O(aRe/M)$ of the non-uniform region although the length in a rectangular duct is somewhat longer than in a circular one. An extensive review of low-N flows in non-uniform fields or in variable area ducts together with a detailed description of their underlying physical principles has recently been published by Branover (1978, chap. 5).

Kit *et al.* (1970) measured velocity profiles in a rectangular duct with a Pitot-static tube as the flow passed through a uniform transverse field. Their results clearly demonstrate that at each end of the magnet the flow hugs the walls parallel to the field, the velocity peaks being more pronounced as M and N increase. Furthermore, as M increases, the velocity maxima formed when the flow approached the magnet can persist to the other end of the magnet and reinforce the effects produced there. It is quite possible for such entrance and exit effects to invalidate calculations and arguments in which they are ignored. For example, Bocheninskii *et al.* (1971) assume that a fully developed flow exists over the central portion of their ducts whereas their measured pressure distributions along the complete duct and some measured velocity profiles clearly show that this assumption is not necessarily true. Consequently their conclusions must be viewed with suspicion.

What experiments that have been done to investigate the type of problem under consideration here have been restricted to variable area ducts with low-N flows, perhaps because, as will become clear later, it is very difficult to achieve high enough values of M to satisfy even the weaker inertialess condition $N \gg M^{\frac{1}{2}}$ and to generate measurable pressure differences. Unfortunately, few investigators have ensured that a fully-developed flow has been realized before and after the non-uniform region; effectively, results are presented in which entrance and exit effects mask the effects being studied. Furthermore, quite often very little thought appears to have gone into what measurements should be taken.

Butsenieks *et al.* (1972) measured the pressure distribution near the step-wise increase in diameter of a circular pipe in a uniform field. Their presented results indicate a pressure *rise* due to the step which is physically impossible. A similar study by Branover, Vasil'ev & Gel'fgat (1967) of the flow in a rectangular duct whose height in the direction of the uniform field suddenly increases is more reliable. Unfortunately, although they measure the fully developed flow pressure gradient in the wide section they do not do so in the narrow section. When reducing their results they choose as a reference pressure the pressure in the wide part of the duct where it does not vary around the perimeter, claiming that fully developed flow must be established there, this can only be regarded as a dubious assumption. However, they do a thorough investigation of the pressure distribution at the step.

Slyusarev, Shilova & Shcherbinin (1970) measured velocity and electric potential distributions inside a diffuser whose pair of tapered walls diverged at $4\frac{1}{2}°$. This was built into the air gap of the magnet and so the field strength decreased along the diffuser. Velocity maxima were observed close to the parallel walls, the effect being more pronounced as the flow travels along the diffuser and as the field strength increases.

Recently, Bocheninskii, Tananaev & Yakovlev (1977) have studied flow in curved tubes, in particular the flow through a 180° bend in a uniform magnetic field. When the field is parallel to the plane of the bend and perpendicular to the straight pipes upstream and downstream of it the problem, in theory, is that of a variable area duct. At the mid point of the bend the flow of current and fluid is parallel to the field and therefore in the vicinity of that point electromagnetic stresses are negligible. Measurements of the pressure distribution for $M = 360$ and $N = 2$ extend for a distance $15a$ downstream of the bend but even then the fully-developed flow pressure gradient is not realised nor is it within a distance of $6a$ upstream of the bend. An estimated pressure drop across the bend is $0{\cdot}3\ \sigma a\ VB_0^2$ or $5{\cdot}6\ \sigma a\ VB_0^2M^{-\frac{1}{2}}$: much larger than anything predicted by H&W. When the field is at right angles to the plane of the bend the flow is clearly disturbed over much the same distances as before and there is still a large pressure drop of about 40 % of that in the previous case. This reflects the nonlinear effects of inertial stresses; if N were very large a symmetric flow with a small pressure drop ought to exist.

The apparatus for the present experiments is described in § 2 and the more obvious limitations it imposes are mentioned. Internal measurements in a circular duct of electric potential and velocity distributions, previously reported by Holroyd (1976) and Hunt & Holroyd (1977), are presented and discussed in § 3.1. Good agreement is found between velocity profiles deduced from the potential measurements and the discrete values measured by hot-film probes. Severe retardation of the flow near the centre of the duct in the non-uniform field region is observed but there is no trace of the novel features predicted by H&W's theory, namely a tube of stagnant fluid and reverse flow. It is argued that viscous and, to a lesser extent, inertial stresses can account for these major differences between theory and experiment. The large bore pipe needed to make these measurements cannot yield satisfactory pressure distributions but a smaller one can do so as is illustrated in § 3.2. Some of these results are also reported by Holroyd & Hunt (1980). Pressure drops due to the non-uniform field of the correct order of magnitude are observed.

In § 4 are described some complementary measurements from a rectangular duct, principally of pressure distributions and the distribution of potential across one of the walls perpendicular to the field in the non-uniform field region. H&W's theory

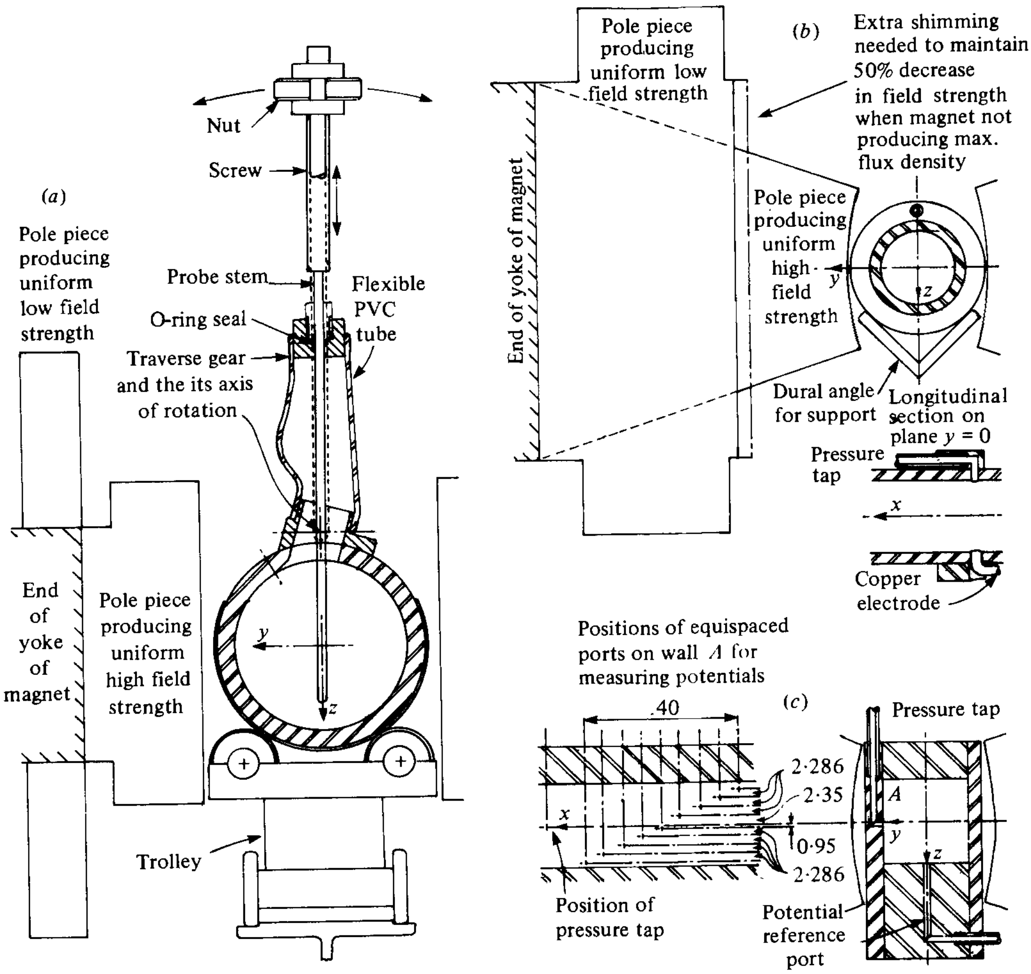

F[illegible]URE 1. Details of ducts: (a) large circular duct showing probe traversing gear and supporting trolley which allows both longitudinal motion and axial rotation; (b) small circular duct; (c) (small) rectangular duct showing positions of ports used to measure potential distribution across wall A. Mean flow is in direction of increasing x.

does not apply to this singular case: indeed a theoretical treatment of it is not available. However, the analogous problem of flow in a straight, rectangular pipe leading into a rectangular diffuser has been analysed by Walker, Ludford & Hunt (1972) and Walker & Ludford (1972). It seems likely that in the non-uniform field region the flow should be confined to boundary layers of thickness $O(aM^{-\frac{1}{2}})$ on the walls parallel to the field lines, so that the velocities there are $O(M^{\frac{1}{2}}V)$. The potential results point to a weak imitation of this prediction. Pressure drops due to the magnetic field of the same order of magnitude as in a circular duct are observed.

Finally in §5 the successes and shortcomings of the experiments are discussed.

2. Experimental apparatus

The 1 m long d.c. electromagnet used in the experiments had a 100 mm thick yoke and a maximum air gap of 200 mm. Pole pieces could be bolted to the facing ends of the yoke to vary the flux density. To optimize the conflicting demands imposed by the ducts described below and others, the first 450 mm of the magnet were used to produce a high strength uniform field to allow in as many cases as possible the appropriate fully developed flow to form in the duct before the region of varying field strength was reached. Over the remaining 550 mm the field strength was 50 % of its high strength value. The shapes of the pole pieces are indicated in figures 1 (*a*) and (*b*). In both cases the variations in flux density over the cross-section of the duct were no more than 3 % of the mean value. For the large duct (figure 1 *a*) the maximum uniform flux density B_0 was 0·56 T and for the smaller ducts it was 1·2 T. Also shown in figure 1 are basic details of the three ducts with their relevant co-ordinate axes namely (*a*) large circular, 78·2 mm I.D. made from ABS and strengthened externally by a 24 s.w.g. stainless steel split tube, (*b*) small PVC circular, 19·48 mm I.D. and (*c*) (small) rectangular 22·225 mm (parallel to field lines) × 22·444 mm, fabricated from perspex sheet. Along each duct fifteen 1·6 mm diameter ports were drilled through the wall to facilitate measurement of pressure distributions and, in the case of the circular ducts, electric potential distributions. In addition, two 10 s.w.g. copper electrodes were inserted through the wall of the small circular tube diametrically opposite to two of the aforementioned ports to provide reference potential points (figure 1*b*). Provision was also made for measuring the potential distribution across one of the walls perpendicular to the field lines in the rectangular duct by drilling a series of ports as shown in figure 1 (*c*). In this case two extra ports in the adjacent wall were used as reference points. The size of the circular ducts was governed by the available sizes of plastic tube which would fit between the pole faces and, in the case of the large duct, minimize the blocking effect on the flow when a probe was inserted. Such an effect may be more important than previously thought; a reduction in cross-sectional area by the probe stem can influence the flow *upstream* of the probe tip (Walker *et al.* 1972) thereby affecting the quantity to be measured. In these experiments the fractional reduction in area was about $M^{-\frac{1}{2}}$ and so the effect should be insignificant.

A flow circuit similar to that used by Shercliff (1956*a*) was used employing mercury as the working fluid. It drained under gravity from one weir tank to a lower one *via* (i) both an electromagnetic flowmeter and the duct and (ii) an overflow pipe and was recirculated by a stainless steel gear pump. Between them the weir tanks and overflow pipe held a constant head of about 1 m of mercury across the circuit which was sufficient to maintain steady flow rates of up to $0{\cdot}15 \times 10^{-3}$ m^3/s through it, regulation of the flow being achieved by PVC ball valves.

Pressure distributions along the ducts were measured with an air-over-liquid-over-mercury manometer system developed by Shercliff (1956*a*). This system increased the numerical value of a pressure difference expressed as a head of mercury by a factor of about 10. In addition, electric potentials at the walls of the ducts were measured *via* the manometer by dipping copper electrodes into the mercury in the standpipes of the system.

Flexible 12·5 mm bore PVC hose was used to interconnect the various items of the flow circuit, thereby allowing movement of the ducts relative to the magnet. Because the flow inside the duct is determined solely by the magnetic field, the positions of the flow inlet and outlet ports are unimportant provided they are remote from the magnet. Therefore it was only necessary to have one port for inserting probes; readings at different points with respect to the field could be made by simply moving the duct and probe. (Note that in this respect corresponding measurements in a variable area duct would be much more difficult to do.) Such axial motion of the ducts was readily achieved by mounting them on a trolley as shown, for example, in figure 1 (*a*).

Internal potential distributions were measured with a probe comprising a 0·5 mm diameter platinum electrode (to minimize the thermoelectric e.m.f. when in contact with the mercury) insulated by PVC sleeve from its 1·78 mm nominal bore stainless steel support tube which was itself insulated from the mercury by PVC sleeving. At one end the tube was sealed with Araldite leaving just the tip of the electrode protruding and about 50 mm above this end the support tube was bent through 45° so that the probe tip would be upstream of its support in the flow. The probe traversing mechanism is sketched in figure 1 (*a*). A simple nut and screw, calibrated in steps of 0·01 mm, moved the probe along a chord of the duct while by suitable rotation of duct and traverse gear support the probe tip could be positioned over a large part of the cross-section.

Velocities were measured with DISA hot-film probes which comprise a nickel film deposited on a quartz rod 70 μm diameter × 3 mm long and insulated from conducting liquids by a 2 μm thick quartz coating. Malcolm (1969*a*, *b*, 1970, 1975) has shown that such probes can be used successfully in MHD experiments subject to some restrictions. The most important problem is the unavoidable contamination of the sensor by impurities in the mercury but this can be overcome by using a modified form of the calibration equation derived by Sajben (1965) which entails taking in rapid succession the sensor readings with the fluid moving (i.e. forced convective heat transfer from the sensor) and with the fluid at rest (i.e. free convective heat transfer). Malcolm showed that free convection is influenced by a magnetic field and so a correcting expression to the calibration equation is required. In this work an adequate correcting expression was derived, similar to the calibration equation, which used the variations in sensor signal for different field strengths when the fluid was at rest. Then, when velocity measurements were made during the experiments, each reading was corrected by an amount which depended on the local flux density which had been measured beforehand. The validity of this procedure was checked by measuring the calibration function at two different field strengths and comparing the difference between them with the correcting expression. Since the anemometer was run in constant temperature mode, the sensor resistance was only affected by the field strength (the magneto-resistive effect) but this can be shown to be negligible (Holroyd 1979*a*).

Calibration of the sensors was carried out in a thick walled copper tube in a uniform field where the velocity profile could safely be assumed to be uniform (see Holroyd, 1979*b*). It is, perhaps, interesting to note that satisfactory results were obtained with hot-film probes even though the mercury used in these experiments had previously been used for other experiments over a period of several months.

Another major problem pointed out by Malcolm is the effect of temperature variations in the fluid. He proposed limiting temperature changes in the fluid to 0·1 K/h

Duct	Characteristic dimension, a (mm)	Max M	Max Re	Max $\sqrt{M}$	Length of high field, region $\times 1/a$	Length of low field, region $\times 1/a$	Duct length, $\times 1/a$	Distance from inlet to first tap $\times 1/a$
Large circular	35·92 (rad)	523	10950	22·9	12·5	15·5	43·7	3·2
Small circular	9·74 (rad)	303	42840	17·4	46·1	57·1	104·6	53·8
Rectangular	11·1125 ($\frac{1}{2}\times$ height)	344	29200	18·5	40·4	50·0	144·0	19·7

TABLE 1

at most; an impractical proposition in the present work. A temperature compensation unit was tried without success. However, satisfactory results were obtained by limiting temperature changes to about 1 K/h by a contrary-flow heat-exchanger and using the mercury temperature in the lower weir tank as a reference value in calculations. In fact, in experiments with the aforementioned copper duct (see Holroyd, 1976, 1979) the heat-exchanger was not used but in that case, unlike the flows in non-conducting ducts, velocity perturbations are less than 15 % of the mean velocity and so significant temperature gradients are not set up between the fluid in the lower wear tank and that near the sensor. In general, half-a-dozen or so measurements of the velocity at some point agreed to within ± 3 % of their mean value.

By comparison, the remaining problems are relatively simple. First, to minimize MHD effects the sensor must be parallel to the field lines; this could be achieved by applying equal and opposite rotations to the duct and traverse gear when necessary. Secondly, flows parallel to the sensor which can seriously affect its signal were eliminated by restricting measurements to the diametral plane about which the field lines were symmetric (i.e. the Oxz-plane in figure 1a) so that $v_y = 0$.

For a detailed discussion of this hot-film probe work and that in the second part of this study (Holroyd 1979b) see Holroyd (1979a).

In table 1 the parameters relevent to the experiments for each duct are summarized. Clearly, in the large circular duct there is insufficient length, in theory, for a fully developed flow to form before the non-uniform field region is reached and this limitation must be borne in mind when interpreting the results.

3. Experiments with the circular ducts

3.1. *Electric potential and velocity measurements*

H&W showed that in a non-conducting duct the maximum value of the current density $|\mathbf{j}| \approx O(M^{-\frac{1}{2}}\sigma|\mathbf{v}\wedge\mathbf{B}|)$ and so it follows from Ohm's law that to $O(1)$ the potential gradient across the duct $\partial\phi\,\partial z$ and the streamwise velocity v_x are related by

$$\partial\phi/\partial z = v_x B_y \qquad (1)$$

on the plane $y = 0$. (The axes are those indicated in figure 1.) In fact, in the larger duct the currents will be slightly larger because they circulate over lengths somewhat shorter than $O(aM^{\frac{1}{2}})$. Nevertheless, they should still be small enough to allow velocity profiles to be deduced from potential distributions. Furthermore, since the potential

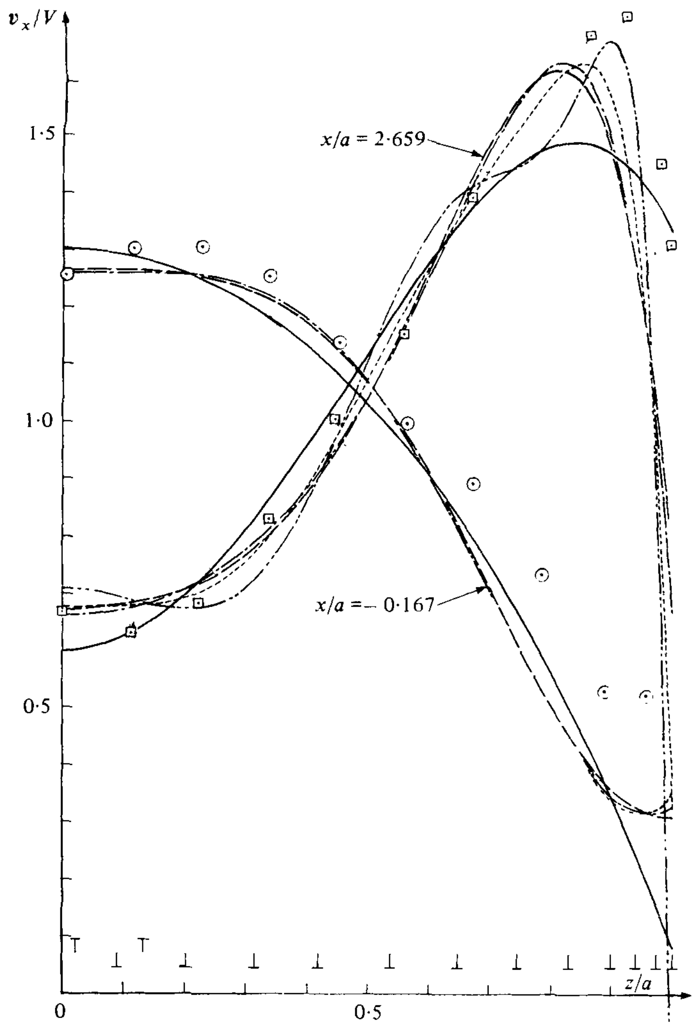

FIGURE 2. Typical results for estimating velocity distributions across duct on the plane $y = 0$. Points ⊙ and ⊡ indicate hot-film probe measurements of velocity. Curves are first differentials of polynomials fitted to measurements of potential distribution across duct. Stations where potentials were measured indicated by ⊥ for $z > 0$ and ⊤ for $z < 0$. Order of polynomials: ——, 5; — —, 7; -·-, 9; ---, 11; ———, 13.

ϕ is constant along a field line (H&W, §3.3) it is possible to estimate the flow rate along the duct from (1) as

$$4\int_0^a\int_0^{(a^2-z^2)^{\frac{1}{2}}}\frac{1}{B_y}\frac{\partial\phi}{\partial z}\,dy\,dz = 4\int_0^a\frac{1}{B_y}(a^2-z^2)^{\frac{1}{2}}\frac{\partial\phi}{\partial z}\,dz. \tag{2}$$

Note that an approximation has been introduced here in that the curvature of the field lines and the slight variations of the flux density B_y in the non-uniform field region have been neglected.

Typical results of such experiments are summarized in figure 2. After measuring the potential distribution at 14 points across the Oxz-centre-plane of the duct with the potential probe, odd-order polynomials were fitted to the data using the leastsquares criterion and then differentiated to give a velocity profile. (Odd-order polynomials were used because the symmetry of the problem implies that ϕ is an odd function of z. The arbitrary datum potential used when making the measurements was represented by a constant term in the polynomials.) When measuring the potentials three readings were taken at each point with different flow rates; the percentage spread of the readings at any point [i.e. (maximum value – minimum value)/mean value] was never more than 6 %. Velocity measurements with the hot-film probe are indicated by the individual points on figure 2 and it can be seen that there is close agreement with the profiles deduced from the potential readings. The mean velocity $V \approx 900/N$ mm/s and so for the range of values of N used in the experiments (66·4–131·6) velocities in the range 1–20 mm/s were successfully measured. That the largest discrepancies should occur near the wall where $v_x \to 0$ is hardly surprising. However, the close proximity of the wall may have some effect on the heat transfer from the sensor but this possibility does not appear to have been explored in hot-film probe studies.

In figure 3 are shown the velocity profiles on the plane $y = 0$ at 12 different positions along the duct.† On this reduced scale the thickness of the contour virtually covers the multitude of curves plotted in figure 2. All readings were taken at the maximum Hartmann number, $M = 523$, and while the potential readings were being taken N varied over the range 66·4–131·6. Values of N at which the hot-film probe readings were made are quoted in the caption to figure 3 along with the position x of the profile relative to the place where the pole pieces and hence the field strength change, the value of $x/aM^{\frac{1}{2}}$, the ratio of the field strength to its value in the high uniform field region and the estimated flow rates derived from (2). The theoretical flow rate is $\pi a^2 V$ and so the maximum fractional error in the estimates is 4·6 %.

An interesting feature of figure 3 occurs in the profile at $x/a = -5{\cdot}178$ – it has a pronounced dip near $z = 0$ which must reflect the effect of the non-uniform field at the upstream edge of the magnet ($x/a = -11{\cdot}8$). After a distance $2a$ downstream the fully-developed flow profile is almost realized but as will be shown later, that is pure chance.

From these velocity profiles, streamlines may be deduced and these are plotted in figure 4 along with the theoretical streamlines in the non-uniform field region deduced from the relationship $\int B^{-1} ds =$ constant, the integration being carried out along field lines inside the duct [H&W, equation (3.3)]. Clearly there is neither stagnant fluid nor reverse flow as was predicted by H&W's theory. On the other hand there is qualitative agreement with their work in that the fluid does migrate towards the centre of the duct upstream of the non-uniform field region before moving outwards fairly rapidly in that region and then slowly migrating back towards a fully-developed flow further along the duct.

In order to explain these differences between theory and experiment it is necessary to recall that H&W's theory begins by assuming that M and N are very large, so that even when their values are effectively reduced to $\frac{1}{2}M$ and $\frac{1}{4}N$ in the low field strength region, viscous and inertial stresses are negligible when compared to the electro-

† In Hunt & Holroyd (1977) 'corresponding' theoretical profiles were indicated on this diagram. Subsequent work discussed here later, but not then available, shows that this is an unfair comparison since the theoretical profiles depend on the boundaries assigned to the non-uniform field region. Data now available show that there is not enough evidence to clearly define such boundaries.

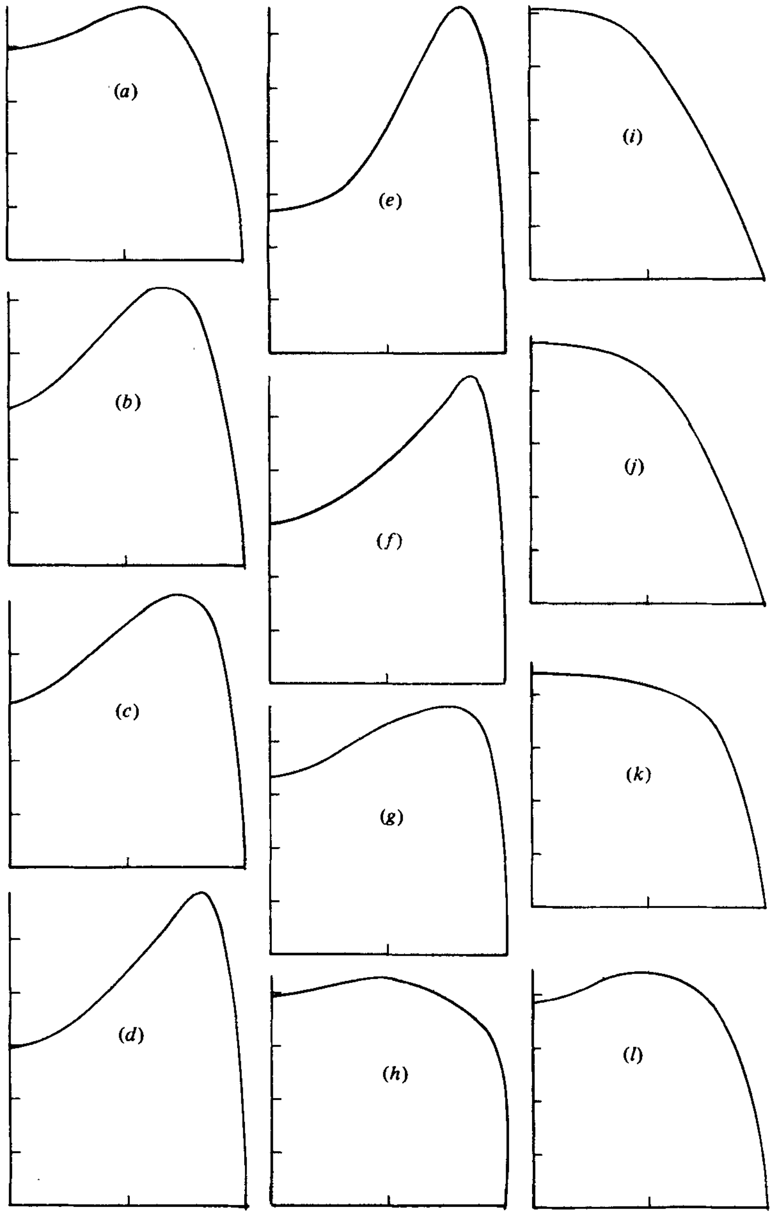

FIGURE 3. For legend see facing page.

magnetic stresses. However, as the effective values of M and N decrease there is a simultaneous increase in the velocity gradients. Therefore, if the flow were to follow the theoretical streamlines shown in figure 4, then at $x/a \approx 4$, for example, the viscous stress term $\eta\, \partial^2 v_x/\partial z^2$ would not be $O(\eta V/a^2)$ but $O(M^2 \eta V/a^2)$ for the value of M in these experiments. Viscous terms of such magnitude are neither catered for in the theory nor apparent in the experimental results. The effects of viscosity will be to reduce the velocity gradients which implies a reduction in the predicted large velocities near the duct walls at $z = \pm a$; therefore to maintain the flow rate along

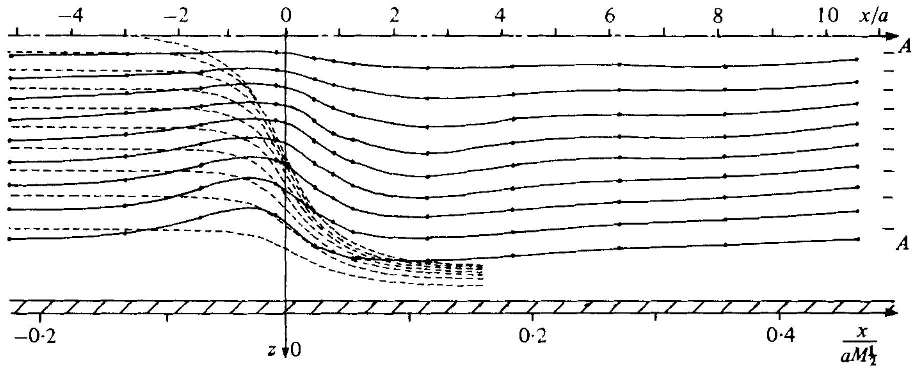

FIGURE 4. Streamlines of flow on plane $y = 0$: —●—, experimental, derived from the velocity profiles in figure 3 whose positions are indicated by the dots; ----, theoretical, derived from the equation $\int B^{-1}ds =$ constant, the integral being carried out along field lines inside the duct [H&W, equation (3.3)]. In both cases there are equal volumes of fluid between adjacent streamlines. The theoretical streamlines start off from a fully developed flow; the short horizontal lines between A–A represent their final (fully-developed flow) positions as $x/a \to \infty$.

the duct there must be forward motion of the fluid near the centre of the duct where it might have been stagnant or flowing backwards.

Inertial effects are probably not as important as viscous effects in altering the predicted flow. In the experiments $N \approx 5M^{\frac{1}{2}}$ so that inertial terms are at most of the same magnitude as the electromagnetic terms.

It follows from these arguments that in the non-uniform field region the flow is governed not only by electromagnetic stresses but also by viscous and inertial stresses.

Although corresponding measurements were not made at the upstream and downstream ends of the magnet, the behaviour of the flow in these regions may be inferred from the distributions of potential measured at the duct wall (via the manometer system) for various orientations of the duct. Such measurements are summarized in figure 5. A reference potential was provided by positioning the tip of the potential

---

LEGEND TO FIGURE 3

FIGURE 3. Summary of measured velocity profiles on plane $y = 0$ for $0 \leqslant |z| \leqslant a$ at $M = 523$. Ordinate axis is v_x/V and each division is 0·2. Axes intersect at centre of duct. Details of profiles are as follows.

	x/a	$x/aM^{\frac{1}{2}}$	B_y/B_0	Flow rate/$\pi a^2 V$	N
(a)	10·636	0·465	0·502	1·045	92·94
(b)	8·185	0·358	0·504	1·016	86·11
(c)	6·245	0·273	0·505	1·017	85·94
(d)	4·257	0·186	0·506	1·0195	92·74
(e)	2·659	0·116	0·525	1·005	132·89
(f)	1·253	0·055	0·636	1·000	147·70/92·34
(g)	0·891	0·039	0·688	0·997	93·09
(h)	0·537	0·0235	0·758	0·996	114·12
(i)	−0·167	−0·007	0·894	1·020	93·24/141·98
(j)	−1·559	−0·068	0·988	1·012	120·85
(k)	−2·979	−0·130	0·994	0·993	92·85
(l)	−5·178	−0·226	0·993	1·005	93·04

The values of N quoted are those at which the hot-film probe measurements were made in each case.

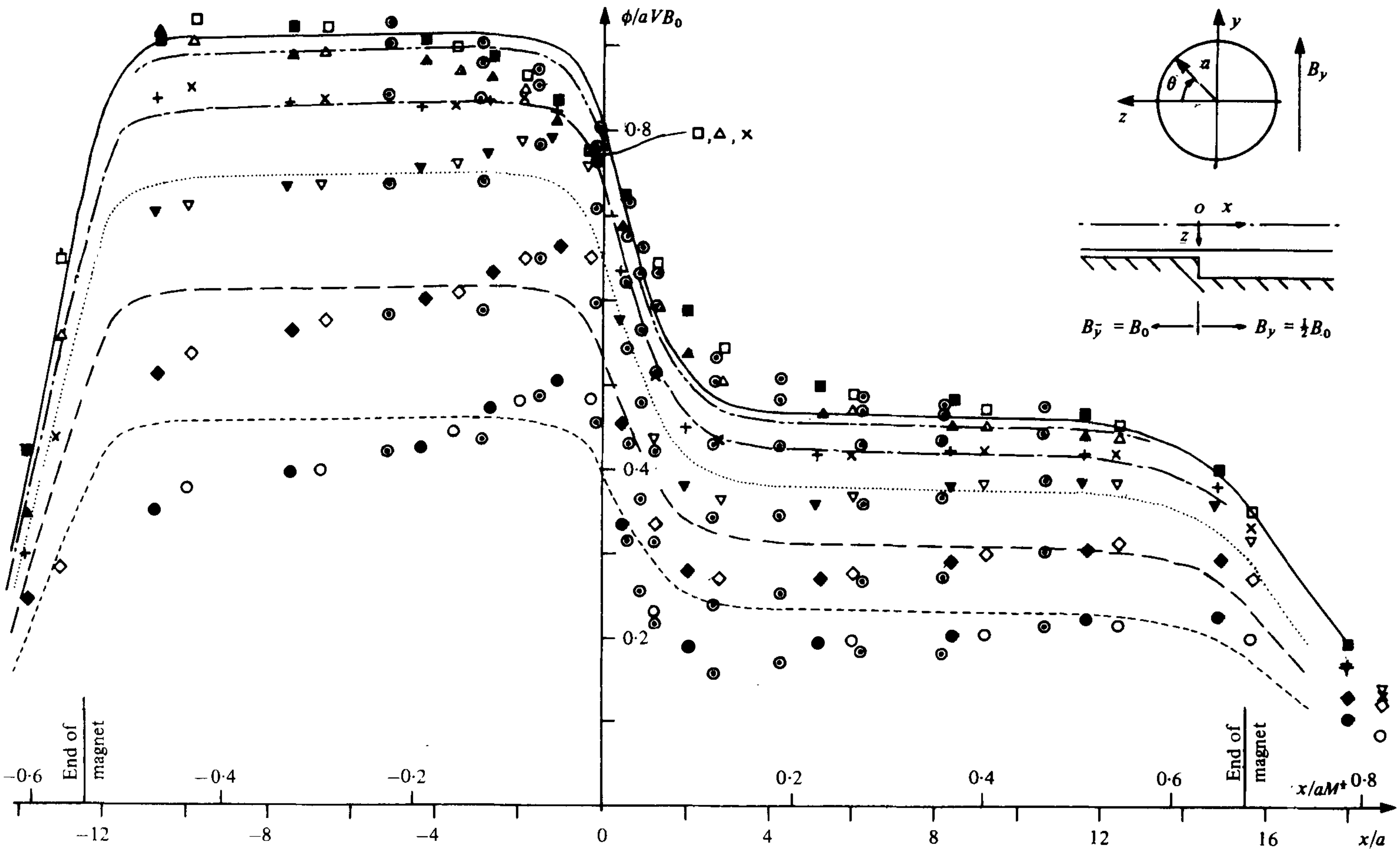

FIGURE 5. Potential at wall of large circular duct measured with respect to axis $y = z = 0$ for $M = 523$, $73 < N < 111{\cdot}4$. Curves indicate corresponding fully-developed flow distributions: ——, $\theta = 0°$, $z/a = 1$; -·-·-·, 20°, 0·940; -·-, 35°, 0·819; ···, 45°, 0·707; —, 56°, 0·559; ---, 66°, 0·407. Points ⊙ represent values derived from potential distributions across duct on plane $y = 0$ (used to derive the velocity profiles of figure 3) by assuming that ϕ does not vary with y. Other symbols indicate results from separate experiments with duct in different positions with respect to the magnet.

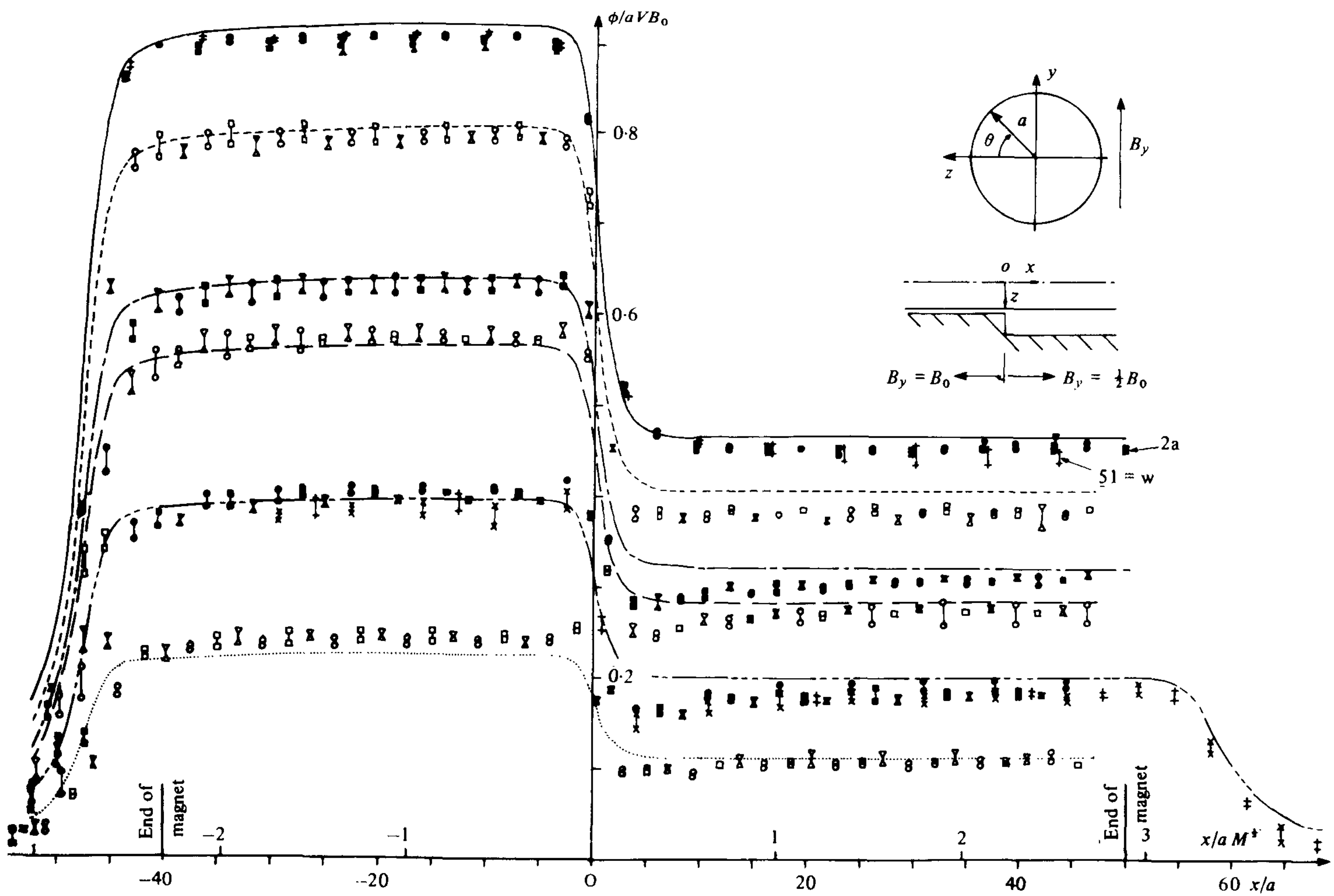

FIGURE 6. Potential at wall of small circular duct measured with respect to axis $y = z = 0$ for $M = 302$, $N = 51$ except when $\theta = 0$ in which case only results indicated by ‡ were measured with $N = 51$; other results were for $N = 29$. Curves indicate fully-developed flow distributions: ——, $\theta = 0°$, $z/a = 1$; - - -, 40°, 0·766; -·-, 55°, 0·574; – –, 60°, 0·5; - - - —, 70°, 0·342; ···, 79°, 0·191. Each symbol represents mean of readings taken with respect to each reference electrode. The two symbols at each point represent measurements at $\pm\theta$.

probe on the axis of symmetry of the duct where theory assumes $\phi = 0$. Readings were limited to $\theta \leqslant 66°$ because the probe traversing gear and pole pieces prevented further rotation of the duct. Points indicated by $\odot$ in figure 5 are derived from the previously discussed potential distributions on the plane $y = 0$ by assuming that ϕ does not vary along the field lines; the close agreement between these points and those measured at the wall supports this theoretical prediction (H&W). To assist the discussion the theoretical distributions for a fully developed flow are plotted on figure 5. By comparing the potential distributions near each end of the magnet with those near $x = 0$ it can be seen that as the flow meets the magnetic field the fluid hugs the walls near $z = \pm a$ as it does immediately downstream of $x = 0$. On the other hand, at the other end of the magnet (where the field strength gradients are much smaller than elsewhere) there is evidence of a velocity maximum at the centre of the duct (at $x/a = 14$) as occurred just before $x = 0$ but no evidence of a subsequent retardation of the flow thereafter.

The distributions in figure 5 clearly show the effects of the relatively short lengths of uniform magnetic field since at no point is there any suggestion of a fully-developed flow being established although at $x/a = -3$ the potential distribution and, as was mentioned earlier, the velocity profile closely approximate to it.

In figure 6 are shown potential distributions along the wall of the small circular duct presented in a similar manner to those in figure 5. The experiments were carried out with $M = 302$ and $N = 51$ ($\approx 3M^{\frac{1}{2}}$). Using a copper electrode as a reference potential ensured that at one point along the duct the potential difference across a diameter was measured. Subtracting half of this value from each of that particular set of readings gave the potential distribution with respect to the axis of symmetry of the duct. Results were checked by taking readings with respect to each of two electrodes. In addition, readings were taken at plus and minus values of θ, the difference being represented by the length of the bar between each pair of symbols in figure 6. The lower value of M ensures that there is sufficient space, in theory, upstream and downstream of the non-uniform field region near $x = 0$ for a fully-developed flow to form and indeed the results do indicate that such a flow is realized over almost the entire high field strength region and near the downstream end of the magnet. Just downstream of $x = 0$ the distributions imply some distortion of the flow but not as severe as that in the larger pipe; obviously the lower Hartmann number necessitates lower velocity gradients in the non-uniform field region and so there can only be small changes in the fully developed velocity profile. However what changes there are do decay over an $O(aM^{\frac{1}{2}})$ distance as predicted by H&W's theory. On the other hand there is no evidence of a velocity peak near the centre of the duct forming over an $O(aM^{\frac{1}{2}})$ length, or even on $O(a)$ length, upstream of $x = 0$.

3.2. *Pressure distributions*

Although the large circular duct was suitable for making internal measurements of the flow it was most unsuitable for measuring reliable pressure distributions. Even at the maximum flow rate available the total pressure drop along it was a mere 0·3 mm of mercury: a value too small to allow accurate and consistent readings to be obtained. The results that were obtained measured at $M = 523$ and $N = 23{\cdot}5$ ($\approx M^{\frac{1}{2}}$), give, at best, only a qualitative description of the pressure distribution along the duct (Holroyd

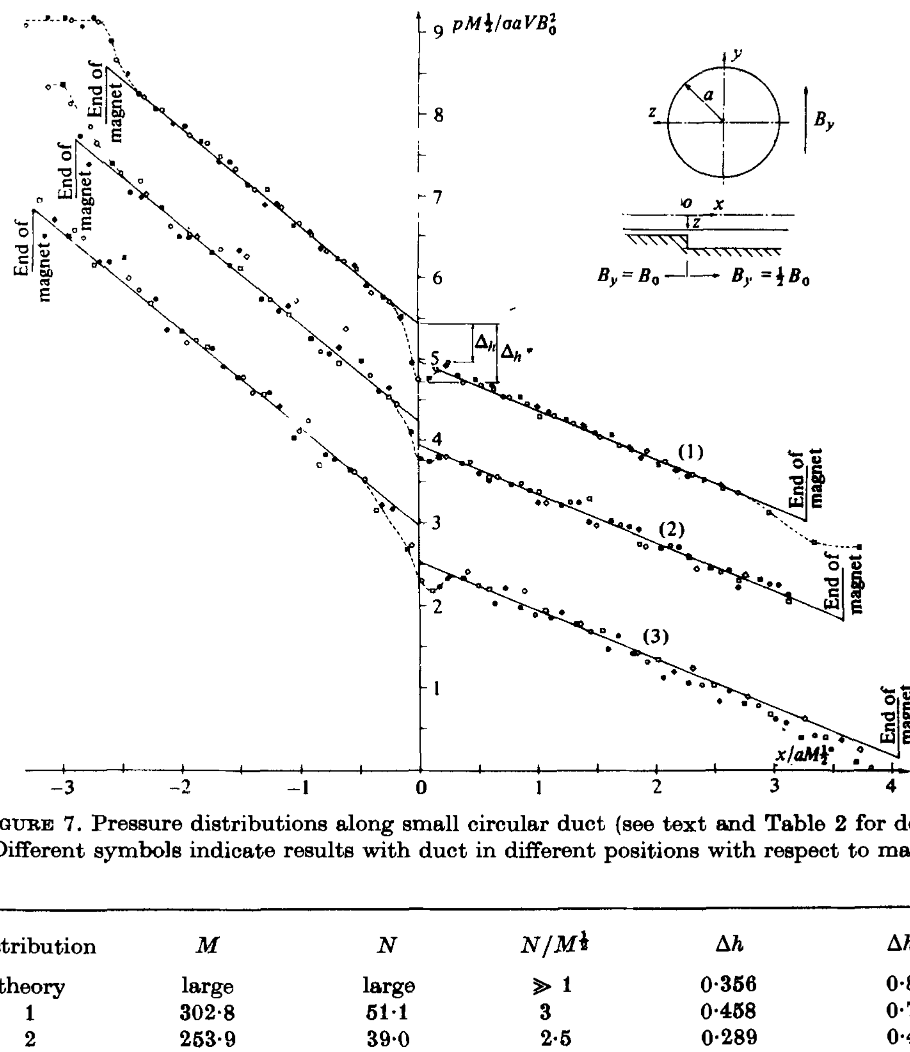

FIGURE 7. Pressure distributions along small circular duct (see text and Table 2 for details). Different symbols indicate results with duct in different positions with respect to magnet.

Distribution	M	N	$N/M^{\frac{1}{2}}$	Δh	Δh^*
theory	large	large	$\gg 1$	0·356	0·83
1	302·8	51·1	3	0·458	0·71
2	253·9	39·0	2·5	0·289	0·49
3	199·5	22·1	1·5	0·435	0·78

TABLE 2

1976; Hunt & Holroyd 1977). Even so, they do exhibit the principal features predicted by H&W, namely a pressure drop of the correct order of magnitude at $x = 0$ and, in that region, a trough whose minimum value is about twice the theoretical value. In addition there is evidence of a somewhat larger pressure drop at the upstream edge of the magnet as well as a local sudden rise and equally sudden fall in the pressure distribution there. Such behaviour can readily be inferred from the available theory.

The small circular duct was designed to overcome this problem. Pressure distributions were measured at three different field strengths and are shown in figure 7; the pressure p measured at $y = a$, $z = 0$ is plotted non-dimensionally as $pM^{\frac{1}{2}}/\sigma a V B_0^2$ against $x/aM^{\frac{1}{2}}$, these being the scales which follow from H&W's theory. Each distribution comprises a visual superposition of distributions measured with the duct in different positions with respect to the magnet. The straight lines represent the fully-developed flow distributions derived from Shercliff (1956*a*) and are also fitted to the data visually. Δh represents the non-dimensional pressure drop and Δh^* the minimum value of the pressure in the trough. Table 2 summarizes the results plotted in figure 7 and H&W's corresponding theoretical results.

Although H&W's condition for an inertialess flow, namely $N \gg M^{\frac{3}{2}}$ is not satisfied there is reasonable agreement between the theoretical and experimental values of the pressure drops and peaks. Further inspection of the distributions in figure 7 shows that the fully-developed flow pressure gradient exists within distances far less than $O(aM^{\frac{1}{2}})$ from the region of non-uniform field but the inevitable scatter in the data presents any accurate assessment of the actual length. In distribution 1 of figure 7 sufficient readings were taken to explore the pressure distribution in the vicinity of the upstream end of the magnet. Although a pressure drop can clearly be defined there is no evidence of a pressure peak contrary to what was observed in the less reliable readings from the larger duct. Here, the non-dimensional value of this drop, 0·856, is somewhat larger than the theoretical value of 0·6.

It was hoped that these three sets of results would clarify the determination of the length of the non-uniform field region. In H&W's theory this region is treated as a discontinuity on the large $O(M^{\frac{1}{2}})$ length scale. However, Holroyd (1976) and H&W suggested that the region might start and end where $|\partial(\int B^{-1} ds)/\partial x| = B_0^{-1} M^{-\frac{1}{2}}$. The available data neither contradicts nor supports this hypothesis since the pressure drop does not increase or decrease monotonically with M. However, it should be noted that whatever value is assigned to the length of the non-uniform field region will slightly increase the value of the pressure drop.

3.3. *The effect of a slowly changing field strength along the duct*

To compare the effects of rate of change of field strength along the duct on the flow Holroyd (1976) measured potential distributions (both internally across the duct and at the wall along it) and pressure distributions in the large duct when the region of low strength field was replaced by a field whose strength decreased in an approximately exponential manner from the high field strength value B_0 to about $0{\cdot}6B_0$ over the last 550 mm of the magnet.

The velocity profiles on the plane $y = 0$ derived from the internal potential measurements show that at $x/a = -5{\cdot}178$ the flow is virtually identical with that shown in figure 3 at the same position, thus supporting the notion that this is a decayed form of the velocity profile formed when the flow meets the magnetic field. However, in this case the dip in this profile near the centre of the duct continues to decay slowly so that even at $x/a = 1{\cdot}25$ (when the field strength is already decreasing) there is still a hint of its presence. The next profile at $x/a = 2{\cdot}66$ resembles that of fully-developed flow although the velocity at the centre is only about 85 % of the fully developed value. Subsequent profiles at $x/a = 5{\cdot}46$ and 8·3 are almost identical and exhibit a dip near $z = 0$. The velocity profiles measured by Slyusarev *et al.* (1970) in their slightly tapered diffuser of rectangular cross-section along which the field strength slowly decreased exhibit a much more pronounced flow near the parallel side walls with a very low velocity flow filling the centre of the duct. Moreover, this effect intensified along the duct. Therefore, the flow in their duct is highly distorted compared to that described here. However, this is not entirely unexpected because if the analyses by Walker & Ludford (1974) and Walker *et al.* (1972) of the flows in expanding circular and rectangular ducts are compared it can be seen that more extreme effects occur in the latter case.

No satisfactory conclusions could be drawn about the pressure distribution in the slowly varying field region but clear evidence of a small pressure trough just downstream of $x = 0$ was observed.

4. Experiments with the rectangular duct

From a theoretical point of view the flow in rectangular duct with a pair of walls parallel to the field lines is a singular case of H&W's theory and so there are no corresponding theoretical results with which to compare the results from these experiments. Some idea of the possible behaviour of the flow in this case can be deduced from analyses by Walker *et al.* (1972) and Walker & Ludford (1972) of the change in a fully developed flow in a rectangular duct as it moves into a rectangular expansion, the field being uniform. In the expansion, which is analogous to the non-uniform field here, the entire flow is initially confined to the boundary layers of thickness $O(aM^{-\frac{1}{2}})$ on the walls parallel to the field lines; the fluid between these layers is stagnant and the streamwise velocity in the layers is $O(M^{\frac{1}{2}}V)$. This extreme velocity profile leads to a much more stricter inertialess condition than that for a circular duct, namely $N \gg M^{\frac{3}{2}}$; clearly this will be extremely difficult if not impossible to realize in practice. Changes in the fully-developed flow upstream of the expansion now occur within a length equal to a few duct heights. For slight divergences of the expansion the extreme velocity profile is relaxed and there is flow over the whole cross-section. As in the circular duct, $|\mathbf{j}|/\sigma|\mathbf{v} \wedge \mathbf{B}| \approx O(M^{-\frac{1}{2}})$ in the core and so the variation in potential across a wall at right angles to the field lines should still provide a reliable guide to the velocity distribution. In addition, there is still a longitudinal recirculating current flow and so pressure distributions should not be unlike those in figure 7. The fully developed flow is described by Shercliff (1953).

Measurements of potential across the wall at $y = a$ in the non-uniform field region are shown in figure 8. Readings were taken with respect to each of the two reference potential ports and the difference in the results is indicated by the length of the bar between the short lines joining the pairs of symbols. All results were taken at the highest available field strength so that $M = 344{\cdot}7$ while N varied between 126·3 and 135·5 ($\approx 0{\cdot}02M^{\frac{3}{2}}$). The nine ports at which potentials were recorded were spread across the whole duct wall at $y = a$ but symmetry allows the values at $z < 0$ to be plotted with a change of sign at the equivalent positions $z > 0$. The corresponding fully-developed flow values are drawn in figure 8. For $x > 0$ the results show that $\partial\phi/\partial z$ is smaller at the centre of the duct than near the wall which implies a velocity profile with a marked dip near $z = 0$ but there is no evidence of any stagnant fluid in the duct. In the circular duct the absence of stagnant fluid at the centre of the duct could be accounted for by viscous effects and, to a lesser extent, inertial effects. Even if stagnant fluid was definitely predicted in this case, the same arguments could not be employed to explain why it did not occur since the analysis, like that of Walker *et al.* (1972), would cater for viscous terms. In fact, inertial effects will play a significant role in attenuating the extreme velocity distribution postulated above since $N \ll M^{\frac{3}{2}}$ here.

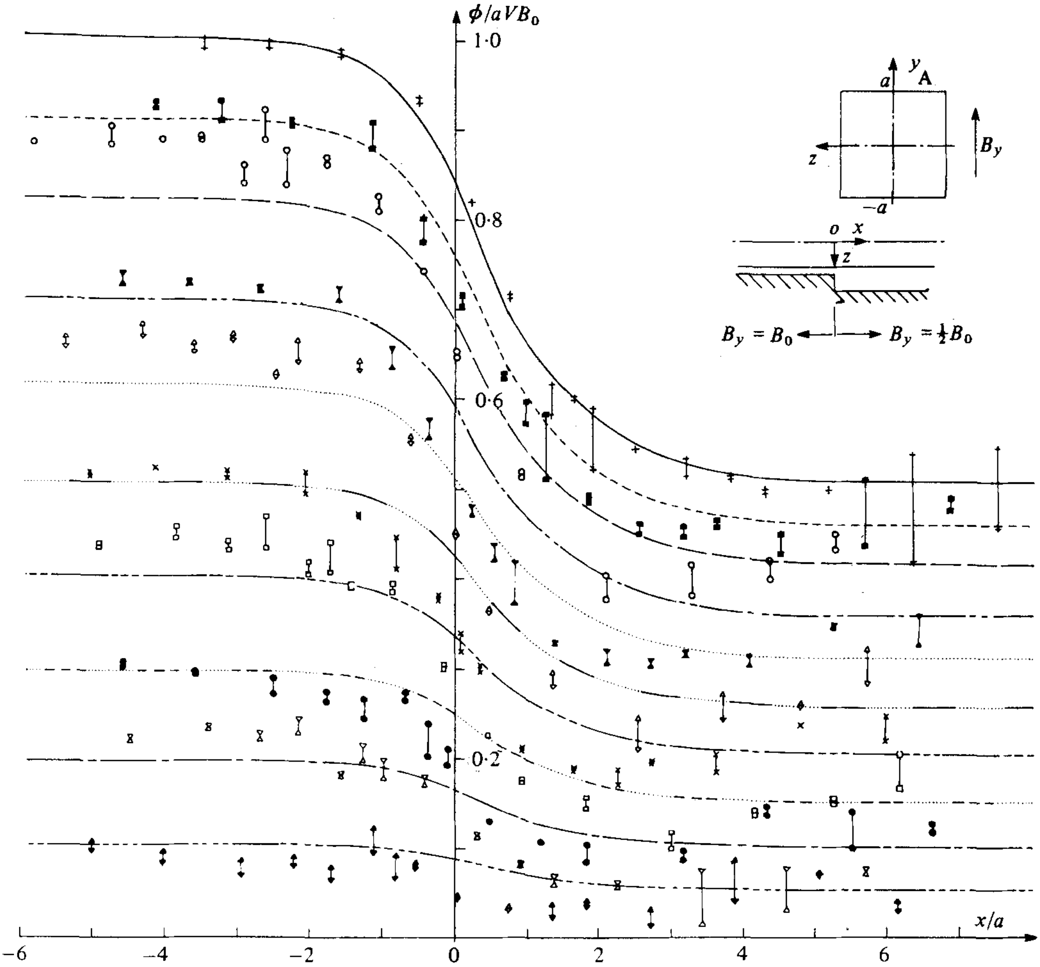

FIGURE 8. Potential distributions across wall A of rectangular duct measured with respect to central axis $y = z = 0$ with $M = 345$, $126 < N < 135{\cdot}5$. Curves indicate fully-developed flow distributions: —+—, $z/a = 1{\cdot}007$; - -■- -, 0·912; —○—, 0·824; - -▼- -, 0·712; ···△···, 0·618; —×···, 0·509; - -□—, 0·404; - -●···, 0·299; -▽-, 0·199; - - -▲—, 0·105; wall at 1·010. The two symbols at each point represent measurements with respect to each reference port.

Pressure distributions along the duct measured at the mid-point of the wall $y = a$ for $M = 343{\cdot}8$, $N = 84{\cdot}9$ ($\approx 0{\cdot}133M^{\frac{4}{3}}$), $Re = 1392$ (1) and $M = 289{\cdot}3$, $N = 72{\cdot}4$ ($\approx 0{\cdot}147M^{\frac{4}{3}}$), $Re = 1158$ (2) are presented in figure 9 and are built up in the same way as those in figure 7. For convenience only, the same scales are used as in figure 7 but sound arguments could be advanced for using others, particularly for the abscissa. It can be seen that the distributions in figure 9 are qualitatively like those in figure 7; there are more pronounced troughs at $x = 0$ with minima of 1·45 and 1·17 in the two cases on the non-dimensional scale used and there are also pressure drops whose non-

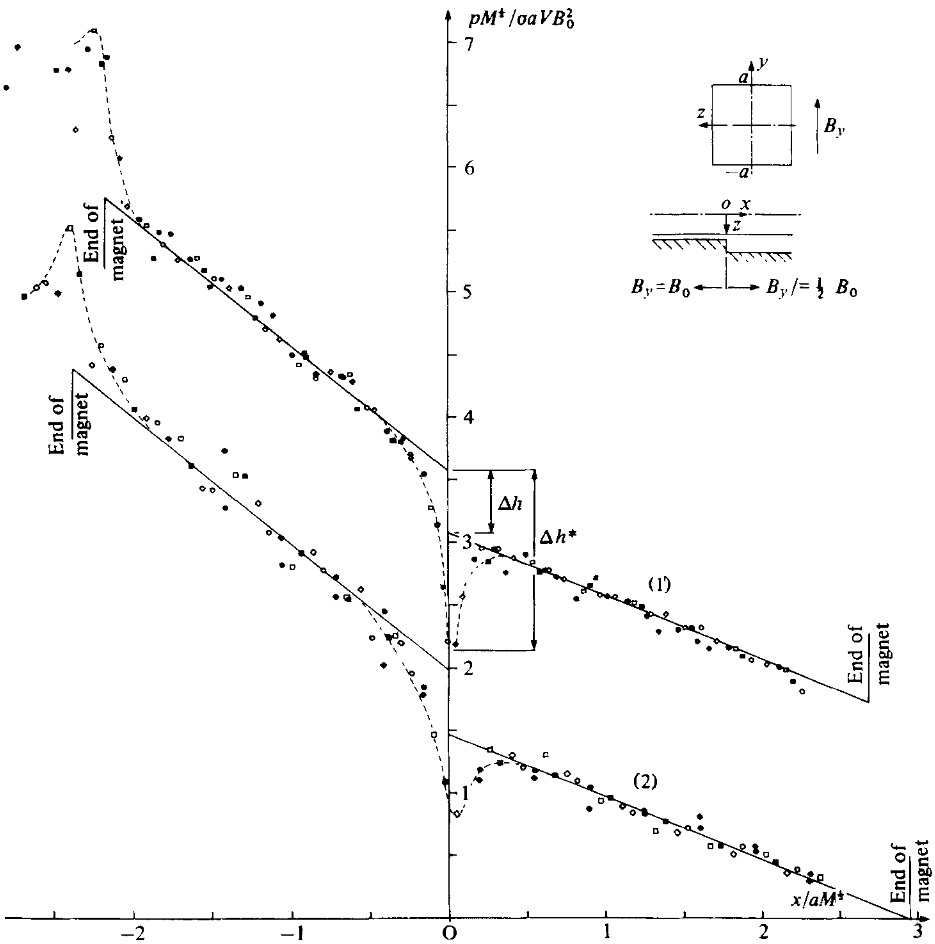

FIGURE 9. Pressure distributions along rectangular duct at $y = a$, $z = 0$ (see text for details). Different symbols indicate results with duct in different positions with respect to magnet.

dimensional values are almost equal, namely 0·52 and 0·5. It is interesting to compare these pressure drops with those that may be estimated from the results of Branover *et al.* (1967) for flow in a rectangular duct with a four-fold increase in cross-sectional area at a step.† Pressure distributions were measured at $Re = 1802$ and values of M, N and the non-dimensional pressure drop $\Delta p \,.\, M^{\frac{1}{2}}/\sigma a V B_0^2$ were 29·55–0·485–106, 20·5–0·233–72 and 11·05–0·068–19. Thus these pressure drops are two orders of magnitude *larger* than those in the present experiments while the interaction parameter and Hartmann number are two orders and one order of magnitude *smaller* respectively. At low values of N some indication of the variation of the pressure drop Δp with N may be deduced from the equation of motion of the fluid [H&W, equation (2.1*a*)] by writing it as

$$\rho \mathbf{v} \,.\, \nabla \mathbf{v} = -\nabla p + \text{electromagnetic term} + \text{viscous term}.$$

† In that paper, pressures are quoted in mm of mercury but only by assuming that they should be cm of mercury can the pressure gradient in the wide part of the duct be reconciled with the theoretical value.

The inertial term is $O(\rho V^2/a)$ since the change in mean velocity occurs over an $O(a)$ length (Shercliff 1956*b*). Therefore

$$\Delta p/\sigma a V B_0^2 \approx O((\rho V^2/a) . a/\sigma a V B_0^2) = O(N^{-1})$$

which agrees qualitatively with these results.

Another interesting feature of the pressure distributions in figure 9 is that the effects of the non-uniform field are expressed over larger distances upstream and downstream of $x = 0$ than in the circular duct (compare with figure 7). So, even though high values of N were attained in these experiments the disturbance (or entry) lengths predicted by Shercliff (1956*a*, *b*) for the two cases still appear to be applicable presumably because the condition for an inertialess flow, namely $N \gg M^{\frac{3}{2}}$, was not realized.

5. Conclusions

In a qualitative sense the experiments have supported prediction of H&W's theory but at the same time they have exposed its limitations and those of the apparatus used.

Clearly the flow in regions of non-uniform field is greatly disturbed but not in the dramatic manner predicted. In circular ducts the potential and velocity readings suggest that the disturbances decay over an $O(aM^{\frac{1}{2}})$ length downstream of the non-uniform field region but this is not confirmed by the pressure distributions. On the other hand, for the rectangular duct the pressure distributions point to a more persistent disturbance upstream and downstream of the non-uniform field region. Such results are more readily reconciled with low-N rather than high-N theories. The predicted peaks, troughs and drops in the pressure distributions are, on the whole, slightly larger than their predicted values. Sound arguments have been advanced which imply that the discrepancies between theory and experiment are a result of the relatively low values of M and N and the difficulty in satisfying the condition $N \gg M^{\frac{1}{2}}$. In other words, the effects of viscosity and inertia which are ignored by theory *cannot* be ignored in practice.

A more thorough test of high-N theory would call for a magnet capable of producing field strengths an order of magnitude greater than those available here over lengths of say $5aM^{\frac{1}{2}}$. Of course, such a magnet would be much longer than any that appear to exist at present.

From a theoretical point of view a coherent theory comparable to that of H&W is required which includes both viscous and inertial terms. Such a theory would enable a much more realistic assessment of laboratory experiments to be made and give a clearer indication of the limitations of high-M and high-N analyses. Both Hunt & Leibovich (1967) and Kapila & Ludford (1975) have derived solutions in which inertial terms appear as a first order perturbation but only for two-dimensional flows with no variation in the direction perpendicular to both the flow and field. However, the usefulness of these results must be questioned since it is doubtful whether such cases can be realized in practice. More recently, El-Consul & Walker (1979) have considered the inertial perturbation in a three-dimensional flow in a non-conducting rectangular duct but again with a limitation which is that the divergence of the duct is small. This, of course, underlines the non-trivial nature of such analyses.

The second part of this study (Holroyd 1979*b*) will include complementary investigations of the flow in (i) a highly-conducting walled (copper) uniform bore tube (pressure and velocities measured), (ii) a uniform bore pipe with weakly conducting walls (only pressure measurements) and (iii) various tubes with weakly conducting walls containing bends, etc. (pressures and potentials measured).

The author would like to thank Dr M. D. Cowley and Dr J. C. R. Hunt for supervising the research work which formed the basis for this paper. He would also like to thank one of the referees for drawing his attention to the presence of magneto-resisitive effects in nickel-plated hot-film probes and the other for pointing out the different inertialess flow conditions for circular and rectangular ducts. While carrying out the research, the author was supported by grants from the Science Research Council and the Culham Laboratory of the United Kingdom Atomic Energy Authority. The experiments with the large circular duct were financed by Culham Laboratory, who also loaned the electromagnet and its motor-generator set and carried out some computational work for the design of the pole pieces for the magnet. The experiments with the small ducts were financed by the S.R.C. The gear pump used in the experiments was loaned by the Department of Engineering, University of Warwick.

REFERENCES

Bocheninskii, V. P., Branover, G. G., Tananaev, A. V. & Chernyaev, Yu. P. 1971 Experimental investigation of the resistance to the flow of a conducting fluid in flat insulated ducts in the presence of a transverse magnetic field with allowance for fringe effects and wall roughness. *Izv. Akad. Nauk. SSSR Mekh. Zhid. i Gaza* **6**, 4, 10.

Bocheninskii, V. P., Tananaev, A. V. & Yakovlev, V. V. 1977 An experimental study of the flow of an electrically conducting fluid along curved tubes of circular cross-section in strong magnetic fields. *Mag. Gidro.* **14**, 4, 61.

Branover, G. G., Vasil'ev, A. S. & Gel'fgat, Yu. M. 1967 Effects of a transverse magnetic field on the flow in a duct at a sudden cross-section enlargement. *Mag. Gidro.* **3**, 3, 99.

Branover, H. 1978 *MHD Flow in Ducts*. Keter Publishing House Jerusalem Ltd. (Israel Universities Press).

Butsenieks, I. E., Gel'fgat, Yu. M., Gudkov, A. L. & Shcherbinin, E. V. 1972 Determination of resistance coefficient of tubes with sharp changes in cross-sectional area in a magnetic field. *Mag. Gidro.* **8**, 3, 51.

El-Consul, A. M. & Walker, J. S. 1979 Inertial perturbations of inertialess MHD flow in insulating rectangular ducts with small divergences. To be published.

Holroyd, R. J. 1976 MHD duct flows in non-uniform magnetic fields. Ph.D. dissertation, University of Cambridge.

Holroyd, R. J. 1979*a* Hot-film probe velocity measurements in liquid metal MHD duct flow experiments. To be published.

Holroyd, R. J. 1979*b* An experimental study of the effects of wall conductivity, non-uniform magnetic fields and variable-area ducts on liquid metal flows at high Hartmann number. Pt. II. Ducts with conducting walls. *J. Fluid Mech.* To be published.

Holroyd, R. J. & Hunt, J. C. R. 1980 Theoretical and experimental studies of liquid metal flows in strong non-uniform magnetic fields in ducts with complex geometry. *Proc. 2nd Bat-Sheva Int. seminar on MHD flows and turbulence.*

Holroyd, R. J. & Walker, J. S. 1978 A theoretical study of the effects of wall conductivity, non-uniform magnetic fields and variable-area ducts on liquid metal flows at high Hartmann number. *J. Fluid Mech.* **84**, 471.

HUNT, J. C. R. & HOLROYD, R. J. 1977 Applications of laboratory and theoretical MHD duct flow studies in fusion reactor technology. *U.K.A.E.A. Res. Group Rep., Culham Lab.* CLM-R169.

HUNT, J. C. R. & LEIBOVICH, S. 1967 MHD flow in channels of variable cross-section with strong transverse magnetic fields. *J. Fluid Mech.* **28**, 241.

KAPILA, A. K. & LUDFORD, G. S. S. 1977 MHD with inertia: flow over blunt obstacles in channels. *Int. J. Eng. Sci.* **15**, 465.

KIT, L. G., PETERSON, D. E., PLANTIEKS, I. A. & TSINOBER, A. B. 1970 Investigation of the influence of fringe effects on a MHD flow in a duct with non-conducting walls. *Mag. Gidro.* **6**, 4, 47.

MALCOLM, D. G. 1969*a* Some aspects of turbulence measurements in liquid mercury using cylindrical quartz-insulated hot-film sensors. *J. Fluid Mech.* **37**, 701.

MALCOLM, D. G. 1969*b* Investigation of a steady MHD shear layer using hot-film anemometry. *Nature* **224**, 909.

MALCOLM, D. G. 1970 MHD effects on hot-film measurements in mercury. *DISA Information* no. 9.

MALCOLM, D. G. 1975 Hot-film anemometry in liquid metal MHD. *Proc. Bat-Sheva Int. Seminar on MHD Flows and Turbulence.* Israel University Press.

SAJBEN, M. 1965 Hot wire anemometer in liquid mercury. *Rev. Sci. Inst.* **36**, 945.

SHERCLIFF, J. A. 1953 Steady motion of conducting fluids in pipes under transverse magnetic fields. *Proc. Cambridge Phil. Soc.* **49**, 136.

SHERCLIFF, J. A. 1956*a* The flow of conducting fluids in circular pipes under transverse magnetic fields. *J. Fluid Mech.* **1**, 644.

SHERCLIFF, J. A. 1956*b* Entry of conducting and non-conducting fluids in pipes. *Proc. Cambridge Phil. Soc.* **52**, 573.

SLYUSAREV, N. M., SHILOVA, E. I. & SHCHERBININ, E. V. 1970 Experimental study of MHD flows in converging and diverging channels. *Mag. Gidro.* **6**, 4, 59.

WALKER, J. S. & LUDFORD, G. S. S. 1972 Three-dimensional MHD duct flows with strong transverse magnetic fields. Pt IV. Fully insulated, variable-area rectangular ducts with small divergences. *J. Fluid Mech.* **56**, 481.

WALKER, J. S. & LUDFORD, G. S. S. 1974 MHD flow in insulated circular expansions with strong transverse magnetic fields. *Int. J. Eng. Sci.* **12**, 1045.

WALKER, J. S., LUDFORD, G. S. S. & HUNT, J. C. R. 1972 Three-dimensional MHD duct flows with strong transverse magnetic fields. Pt III. Variable-area rectangular ducts with insulating walls. *J. Fluid Mech.* **56**, 121.